Elastic scattering of low-energy electrons by nitromethane

A. R. Lopes, S. d'A. Sanchez, and M. H. F. Bettega
Departamento de Física, Universidade Federal do Paraná, Caixa Postal 19044, 81531-990 Curitiba, Paraná, Brazil
(Received 4 March 2011; published 27 June 2011)

In this work, we present integral, differential, and momentum transfer cross sections for elastic scattering of low-energy electrons by nitromethane, for energies up to 10 eV. We calculated the cross sections using the Schwinger multichannel method with pseudopotentials, in the static-exchange and in the static-exchange plus polarization approximations. The computed integral cross sections show a π^* shape resonance at 0.70 eV in the static-exchange-polarization approximation, which is in reasonable agreement with experimental data. We also found a σ^* shape resonance at 4.8 eV in the static-exchange-polarization approximation, which has not been previously characterized by the experiment. We also discuss how these resonances may play a role in the dissociation process of this molecule.

DOI: 10.1103/PhysRevA.83.062713 PACS number(s): 34.80.Bm, 34.80.Gs

I. INTRODUCTION

In recent studies of molecular physics, one of the major interests concerns the formation of resonances that would be responsible for molecular dissociation. Boudaïffa *et al.* [1] discovered that low-energy electrons can cause single and double strand breaks in DNA by forming transient states with the constituents. This process is known as dissociative electron attachment (DEA). An important step toward understanding how dissociation occurs is the correct characterization of the resonances involved in DEA. In a direct pathway, the electron is attached to a σ^* resonance, leading directly to dissociation. In the indirect pathway, the electron is first captured in a π^* orbital, which is then connected to a dissociative σ^* resonance. In the latter process, symmetry breaking to couple these resonances is required. Determining which is the correct pathway is not an easy task, since it requires elaborate nuclear dynamics calculations. This was clearly observed in the recent discussion in the literature concerning the formic acid molecule [2–5].

Information on dissociative electron attachment to systems such as DNA constituents is not easily obtained due to the size of the molecules involved. Hence, we chose to investigate the DEA process in a simpler, but also highly polar molecule, in this work, like nitromethane. The nitromethane (CH_3NO_2) molecule is the simplest nitro-organic compound. It may serve as an explosive and propellent [6], and it may also play an important role in atmospheric chemistry [7]. Due to its rich and complex chemistry, it has been widely studied by several groups and techniques. A feature of great interest, and the focus of this work, is the fact that it can easily form a transient negative ion (TNI). The TNI formation was investigated, for instance, by photodissociation processes [8], photoelectron imaging spectroscopy [9], electron transfer from alkali-metal atoms [10], electron transmission spectroscopy (ETS) [11], and DEA spectroscopy [11–15].

Modelli and Venuti [11] studied nitromethane using both ETS and DEA spectroscopy. The ET spectra presented a sharp feature at around 0.45 eV, associated with the capture of an electron in an empty π^* orbital, and a broad feature [2.8 eV full wave at half maximum (FWHM)] at 4.0 eV. Their DEA studies observed only a NO_2^- fragment at 0.6 eV, being related to the π^* resonance previously found, indicating that this resonance follows a dissociative decay channel.

Walker and Fluendy [13] performed DEA experiments, along with electron and optical scattering methods, to investigate the low-lying anionic states of nitromethane. They found anionic states around 0.72, 2.4, 4.0, 5.6, 6.1, and above 8 eV. They associated the first and second (considering vibrational excitations for the latter) to π^* and σ^* orbitals, respectively. They stated that these two resonances are along the C–N coordinate, with the former being strongly bonding while the latter having an antibonding character. Dissociation then occurs in an indirect pathway due to curve crossing of these two resonances. Higher-energy peaks were harder to address, where involvement of excited states was speculated.

Sailer *et al.* [14] performed DEA measurements on nitromethane, showing that several different ions can be produced. The strongest peak observed was from the NO_2^- fragment at 0.62 eV. This peak was assigned to the formation of a π^* shape resonance at the N = O bond with antibonding character. The formation of this fragment, however, requires energy transfer from the N = O to the C–N bond. The same fragment was also observed at energies ranging from 3 to 6 and around 8 eV. According to the authors, electronic excited transient ions (core-excited shape resonances) would be responsible for the dissociation at higher energies. The same group revisited this experiment using a high mass-resolution sector field instrument [15]. Due to its improved resolution, the energies of NO_2^- dissociation peaks were set at 0.5 and 4.5 eV, though their explanation of the dissociation paths remained the same.

To the best of our knowledge, however, there is only one study on electron scattering by nitromethane. In their experiment, Lunt *et al.* [16] measured integral scattering cross sections from 30 meV to 1 eV. They did not observe any resonance structure in this energy range, probably due to the large dipole moment of the molecule.

To fully characterize a TNI, one needs to look at the scattering cross sections in order to obtain positions and widths for the different types of resonances. Hence, the purpose of this paper is to characterize the resonances of nitromethane by performing scattering calculations at the equilibrium ground-state geometry, since there are only DEA,

ETS, and very low-energy integral cross-section data available in the literature. To obtain DEA cross sections, one would require scattering calculations at several different molecular geometries, which is not the goal of this study. We used the Schwinger multichannel method with pseudopotentials to compute the cross sections up to 10 eV and properly identified a π^* resonance at 0.7 eV and a σ^* resonance at 4 eV, not clearly addressed in previous works.

This paper is organized as follows. In Sec. II, we present a brief description of the theoretical formulation and the computational procedures. In Sec. III, we present our results and discussion. At the end, we present a brief summary of our conclusions.

II. THEORY AND COMPUTATIONAL DETAIL

The Schwinger multichannel (SMC) method [17–19] and its implementation with pseudopotentials (SMCPP) [20] have been described in detail in several publications. Here, we will only describe the relevant points concerning the present work. The SMC method is a variational method that results in the following expression for the scattering amplitude

$$f(\mathbf{k_f},\mathbf{k_i}) = -\frac{1}{2\pi}\sum_{m,n}\langle S_{\mathbf{k}_f}|V|\chi_m\rangle(d^{-1})_{mn}\langle\chi_n|V|S_{\mathbf{k}_i}\rangle, \quad (1)$$

where

$$d_{mn} = \langle\chi_m|A^{(+)}|\chi_n\rangle \quad (2)$$

and

$$A^{(+)} = \frac{\hat{H}}{N+1} - \frac{(P\hat{H}+\hat{H}P)}{2} + \frac{(PV+VP)}{2} - VG_P^{(+)}V. \quad (3)$$

In the above equations, $|S_{\mathbf{k}_{i,f}}\rangle$ is a solution of the unperturbed Hamiltonian H_0 and is a product of a target state and a plane wave, V is the interaction potential between the incident electron and the target, $\{|\chi_m\rangle\}$ is a set of $(N+1)$-electron Slater determinants [configuration state functions (CSFs)] used in the expansion of the trial scattering wave function, $\hat{H} = E - H$ is the total energy of the collision minus the full Hamiltonian of the system, with $H = H_0 + V$, P is a projection operator onto the open-channel space defined by the target eigenfunctions, and $G_P^{(+)}$ is the free-particle Green's function projected on the P space. The configuration space in the static-exchange (SE) approximation is constructed as

$$\{|\chi_m\rangle\} = \{\mathcal{A}(|\Phi_1\rangle \otimes |\varphi_m\rangle)\}, \quad (4)$$

where $|\Phi_1\rangle$ is the target ground-state wave function, described at the Hartree-Fock level of approximation, $|\varphi_m\rangle$ is a one-electron function, and $\mathcal{A}$ is the antisymmetrization operator. For calculations in the static-exchange plus polarization (SEP) approximation, the above set is augmented by including CSFs constructed as

$$\{|\chi_m\rangle\} = \{\mathcal{A}(|\Phi_m\rangle \otimes |\varphi_n\rangle)\}, \quad (5)$$

where $|\Phi_m\rangle$ are N-electron Slater determinants, which are obtained by performing single excitations from the occupied (hole) orbitals to a set of unoccupied (particle) orbitals. To take polarization effects into account, we employed the improved virtual orbitals (IVOs) [21] to represent particle and scattering orbitals.

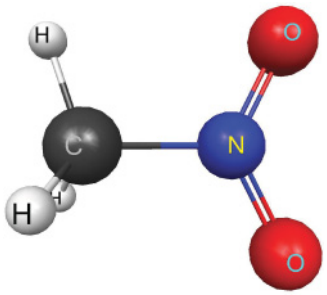

FIG. 1. (Color online) Geometric structure of CH_3NO_2 molecule (generated using McMolPlt [23]). The geometry is r(C–H) = 1.088 Å, r(C–N) = 1.489 Å, r(N = O) = 1.224 Å, ⟨(HCN) = 107.2°, and ⟨(ONO) = 125.3°.

The target ground state was described in the Hartree-Fock approximation at the experimental equilibrium geometry [22]. The nitromethane belongs to the C_s point group, and its structure is shown in Fig. 1. We used the pseudopotentials of Bachelet, Hamann, and Schlüter [24] to replace the core electrons of carbon, nitrogen, and oxygen. The one particle basis set used to represent the target ground state and the scattering orbitals for carbon, nitrogen, and oxygen has $5s4p2d$ uncontracted Cartesian Gaussian functions and was generated according to Ref. [25]. For hydrogen, we employed the $4s/3s$ basis set generated by Dunning [26], augmented with one p-type function with its exponent equal to 0.75. The symmetric combinations of the d-type functions were not included in our calculations to avoid linear dependency in the basis set.

We employed IVOs [21] with energies less than 1 hartree to represent particle and scattering orbitals. We considered all singlet-coupled and triplet-coupled excitations, retaining only doublets [27], and obtained 6215 CSFs for A' symmetry. In order to avoid overcorrelation, we considered only singlet-coupled excitations for the A'' symmetry, obtaining 2784 CSFs.

To analyze the origin of some structures seen in our computed cross section, we employed a procedure developed by Chaudhuri *et al.* [28], as implemented to electron-molecule collisions according to [27]. By removing a few CSFs of the A' symmetry, we were able to find out that some structures in its cross sections were related to numerical instabilities and are, in fact, spurious. However, there is one structure in the cross section of this symmetry that remains stable under this approach (see below).

The nitromethane has a permanent dipole moment. Hence, long-range interactions are important. The computed dipole moment for nitromethane is 4.21 D, which is greater than the experimental value of 3.46 D [29]. To take the long character of the dipole interaction into account, we employed the Born closure procedure described in [30] to compute the differential cross sections. The lower partial waves of the scattering amplitude (up to an angular momentum $\ell = \ell_{\mathrm{SMC}}$) are described with the SMC approach and the higher ones ($\ell > \ell_{\mathrm{SMC}}$) with the Born approximation for the dipole moment potential. In our calculations, we used $\ell_{\mathrm{SMC}} = 1$ up to 1 eV,

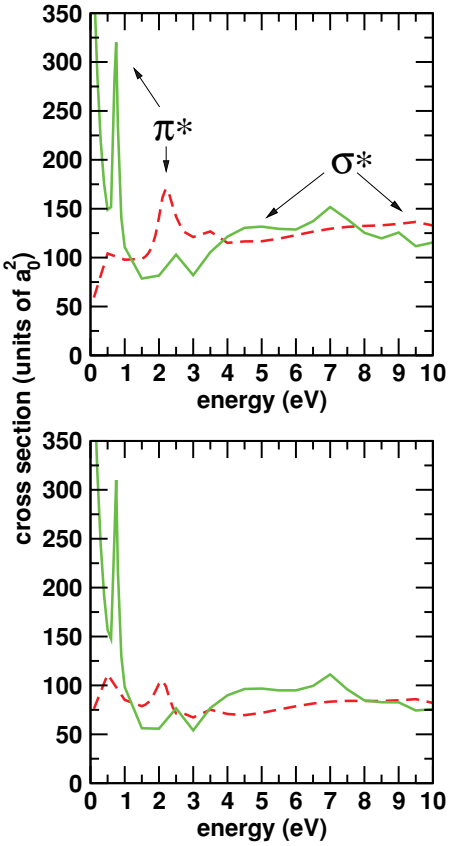

FIG. 2. (Color online) (Upper panel) Integral and (Lower panel) momentum transfer cross sections for CH_3NO_2. Dashed (red) lines, results in the SE approximation; solid (green) lines, results in the SEP approximation. The arrows indicate only the physical π^* or σ^* resonances present in the integral cross sections. Cross sections are in units of a_0^2, where a_0 is the Bohr radius and $1a_0 = 0.529\,18 \times 10^{-10}$ m.

$\ell_{\mathrm{SMC}} = 3$ up to 3 eV, and $\ell_{\mathrm{SMC}} = 5$ at 5, 7, 8, and 10 eV. These values were chosen to minimize the differences between the differential cross sections (DCS) obtained with and without the Born correction at large scattering angles. We have not included the Born closure to integral and momentum transfer cross sections since it could mask the resonances, which are the focus of this work.

III. RESULTS

In Fig. 2, we present integral and momentum transfer cross sections for nitromethane in the SE and in the SEP approximations. In the SE calculations, we found shape resonances at 2.2 and at 9 eV. With the inclusion of polarization effects, these resonances moved to 0.7 and 4.8 eV, respectively. The other structures are pseudoresonances associated with channels that are closed above their thresholds.

The symmetry decomposition shown in Fig. 3 for the SE (SEP) results confirms the π^* character of the 2.2 (0.7) eV resonance and the σ^* character of the 9 (4.8) eV resonance. We also investigated the major partial waves contribution to the resonances from the A' and A'' symmetry in SE and SEP approximations. For the A' symmetry, a combination of $\ell = 2$ and $\ell = 3$ partial waves is associated with the resonance, and

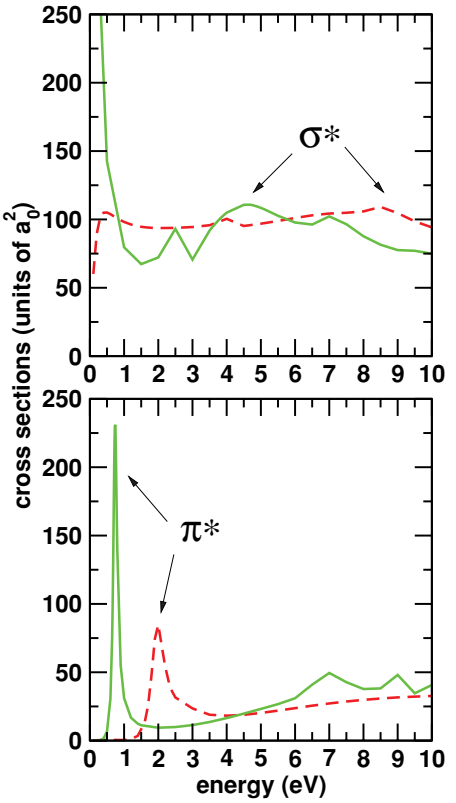

FIG. 3. (Color online) Symmetry decomposition of the integral cross sections for CH_3NO_2. (Upper panel) A' symmetry and (Lower panel) A'' symmetry. Dashed (red) lines, SE results; solid (green) lines, SEP results. The arrows indicate only the physical π^* or σ^* resonances present in the integral cross sections. Cross sections are in units of a_0^2, where a_0 is the Bohr radius and $1a_0 = 0.529\,18 \times 10^{-10}$ m.

for the A'' symmetry, the partial wave associated with the resonance is $\ell = 1$.

As mentioned previously, we have found a structure in the cross section of the A' symmetry below 1.5 eV that comes from $\ell = 1$ (it vanishes at 0 eV). This structure remains stable under the approach used to deal with numerical instabilities discussed above and also for a different basis set. We computed the $\ell = 1$ eigenphase and found no evidence that this structure is a physical resonance.

Figure 4 shows the cross section for the $\ell = 1$ partial wave and the corresponding eigenphase. A similar behavior, considered merely as an angular momentum barrier effect, was also found in positron collisions with CO_2 [31].

In order to investigate if the inclusion of the triplet-coupled excitations is necessary, which could bring overcorrelation to our calculations, we used the procedure proposed by Winstead and McKoy [32], which avoids this effect. We used a modified virtual orbital (MVO) [33] obtained from a cationic Fock operator with a charge of +6. We considered only single excitations that preserved the spatial and spin symmetries of the ground state, and used only the MVO as a scattering orbital to build the configuration space. Within this approach, the π^* resonance is located at 0.83 eV, which is close to the 0.7 eV initially reported. This may indicate that the inclusion of the triplet-coupled excitations in the configuration space of the

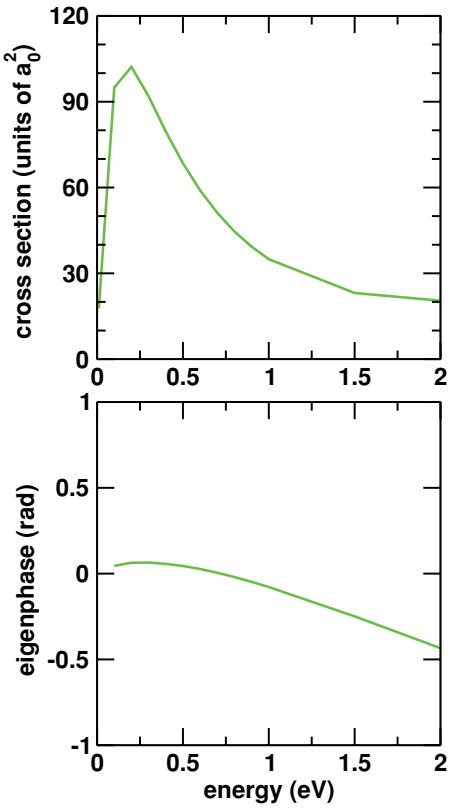

FIG. 4. (Color online) (Upper panel) Cross section and (Lower panel) eigenphase for $\ell = 1$ from the A' symmetry for electron scattering by nitromethane in the SEP approximation. Cross sections are in units of a_0^2, where a_0 is the Bohr radius and $1a_0 = 0.529\,18 \times 10^{-10}$ m.

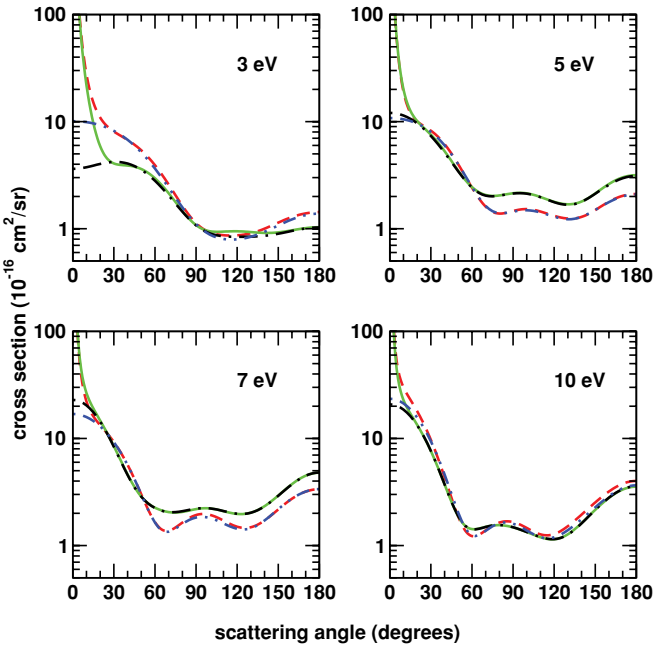

FIG. 5. (Color online) Differential cross sections at 3, 5, 7, and 10 eV for CH_3NO_2. Dashed (red) line, SE results with Born; dot-dot-dashed (blue) line, SE results without Born; solid (green) line, SEP results with Born; dot-dashed (black) line, SEP results without Born.

A'' symmetry results in the overcorrelation of the resonance's position.

In Fig. 5 we show the differential cross sections at 3, 5, 7, and 10 eV for nitromethane obtained in the SE and SEP approximations. We compare our results with and without the Born closure of the dipole potential. The effect of the long-range potential is seen at low scattering angles, where the cross section is forward peaked.

We also carried out electronic structure calculations using GAMESS [34]. We optimized the geometry at the Hartree-Fock level using the 6-31G(d) basis set, and, at this geometry, computed the energy and the molecular orbitals. Figure 6 shows the plots of the lowest unoccupied molecular orbital (LUMO) and the LUMO + 3 molecular orbitals of nitromethane. The LUMO corresponds to an a'' molecular orbital, which is concentrated on the double bonds (NO_2 moiety). The LUMO + 3 corresponds to a σ^* (a') molecular orbital and is concentrated on the C–N bond. We also computed the canonical eigenvalues of the Fock operator and, using the empirical scaling relations for the LUMO (π^*) and LUMO + 1 (σ^*) orbitals from [35], we found for the LUMO and for the LUMO + 3, the values 0.39 and 4.60 eV for the vertical attachment energies (VAE), respectively, which are close to the present calculated π^* and σ^* resonance positions. We also computed the σ^* VAE using another scaling relation from [36] for the LUMO, and obtained 4.61 eV. These results indicate that the use of these relations for the LUMO + 3 would give a fair result. We also computed the canonical eigenvalues of the Fock operator using the 6-31G(d) basis set at the experimental geometry used in the scattering calculations. The LUMO and LUMO + 3 orbitals obtained at this geometry still correspond to π^* and σ^* orbitals with the same shape as shown in Fig. 6. Using the scaling relations of [35], the values for the π^* and σ^* VAE were 0.03 and 4.42 eV, respectively. In particular, the value of 0.03 eV for the π^* orbital is much lower than the one previously obtained. These scaling relations, however, were obtained for an optimized geometry at a particular level of approximation and for a particular basis set, and, therefore, these values may be meaningless.

IV. DISCUSSION

The present calculations give the π^* resonance position at 0.7 eV, a little higher when compared to the ETS data of Modelli *et al.* [11] of 0.45 eV. The DEA peak observed for the NO_2^- fragment is located between 0.5 and 0.72 eV [11,13–15], which is inside the experimental error of the resonance reported by [11] and close to the present computed value. As shown in Fig. 6, this resonance is concentrated in the NO_2 moiety and is probably responsible for capturing the electron, initiating the dissociation process for this fragment at this energy range.

These calculations place the σ^* resonance at 4.8 eV, which is much higher in energy than the one found at 2.4 eV in [13]. This value, however, is close to another anionic state observed in the same work (4.0 eV) and to the broad feature shown in [11], also at 4.0 eV. Besides, the results obtained from the scaling relations of Refs. [35,36] suggest that the present

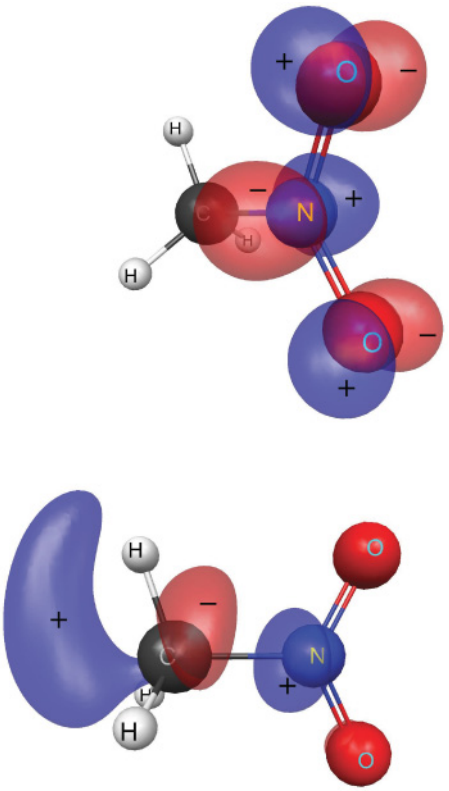

FIG. 6. (Color online) Plots for (Upper panel) the LUMO for a π^* orbital, and (Lower panel) the LUMO + 3 from a σ^* orbital (generated using McMolPlt [23]).

calculations have located the σ^* resonance at the right position. At the fixed nuclei approximation, there is no evidence of a σ^* resonance at 2.4 eV. The energy transfer from the N–O to the C–N bond that causes dissociation probably occurs through the crossing between the π^* and the σ^* (which is concentrated at C–N bond, as shown in Fig. 6) potential energy surfaces. These results corroborate the fact that the strong DEA peak observed for the NO_2^- fragment may be due to an indirect dissociation pathway, as suggested in [13,14].

The presence of a σ^* resonance at C–N bond can also account for the small NO_2^- dissociation peak seen at 4.5 eV [15]. Although core excited resonances may play an important role in DEA at those energies, a direct pathway for NO_2^- formation is also possible, with the electron being captured directly by the σ^* resonance. However, in both cases, DEA calculations are important.

V. SUMMARY

We presented elastic cross sections for electron collisions with CH_3NO_2. These calculations, in the static-exchange plus polarization approximation, show a π^* shape resonance around 0.70 eV and a σ^* shape resonance at 4.8 eV, in agreement with experimental data.

The present results corroborate the experimental evidence that the strong DEA peak observed for the NO_2^- fragment may be through an indirect dissociation pathway, due to a possible crossing of the π^* and σ^* resonances. Although proper DEA calculations are required, it is also possible that a direct dissociation takes place, with the electron being captured by the σ^* resonance.

It is possible to observe from the results presented in this paper that there are similarities between formic acid and nitromethane, since there could be two possible mechanisms of DEA. However, to determine the correct pathway, it is required to do elaborate calculations of the nuclear dynamics, which was not the main purpose of this work.

ACKNOWLEDGMENTS

The authors acknowledge support from the Brazilian agency Conselho Nacional de Desenvolvimento Científico e Tecnológico (CNPq). MHFB acknowledges support from the Paraná State agency Fundação Araucária and from FINEP (under Project CT-Infra 1), and also computational support from Professor Carlos M. de Carvalho at Departamento de Física, UFPR. The calculations were carried out at DF-UFPR and CENAPAD-SP.

[1] B. Boudaïffa, P. Cloutier, D. Hunting, M. A. Huels, and L. Sanche, Science **287**, 1658 (2000).
[2] G. A. Gallup, P. D. Burrow, and I. I. Fabrikant, Phys. Rev. A **79**, 042701 (2009).
[3] T. N. Rescigno, C. S. Trevisan, and A. E. Orel, Phys. Rev. Lett. **96**, 213201 (2006).
[4] T. N. Rescigno, C. S. Trevisan, and A. E. Orel, Phys. Rev. A **80**, 046701 (2009).
[5] G. A. Gallup, P. D. Burrow, and I. I. Fabrikant, Phys. Rev. A **80**, 046702 (2009).
[6] Y. A. Gruzdkov and Y. M. Gupta, J. Phys. Chem. **102**, 8325 (1998).
[7] W. D. Taylor, T. D. Allston, M. J. Moscato, G. B. Fazekas, R. Kozlowski, and G. A. Takas, Int. J. Chem. Kinetics **12**, 231 (1980).
[8] D. J. Goebbert, D. Khuseynov, and A. Sanov, J. Chem. Phys. **133**, 084311 (2010); D. J. Goebbert, K. Pichugin, and A. Sanov, *ibid.* **131**, 164308 (2009) and references therein.
[9] C. L. Adams, H. Schneider, K. M. Ervin, and J. M. Weber, J. Chem. Phys. **130**, 074307 (2009).
[10] P. R. Brooks, P. W. Harland, and C. E. Redden, J. Am. Chem. Soc. **128**, 4773 (2006) and references therein.
[11] A. Modelli and M. Venuti, Int. J. Mass Spectrom. **205**, 7 (2001).
[12] A. Di Domenico and J. L. Franklin, Int. J. Mass Spectrom. Ion Phys. **9**, 171 (1972).
[13] I. C. Walker and M. A. D. Fluendy, Int. J. Mass Spectrom. **205**, 171 (2001).
[14] W. Sailer, A. Pelc, S. Matejcik, E. Illenberg, P. Scheier, and T. D. Mark, J. Chem. Phys. **117**, 7989 (2002).

[15] E. Alizadeh, F. F. Silva, F. Zappa, A. Mauracher, M. Probst, S. Denifl, A. Bacher, T. D. Mark, P. L. Vieira, and P. Scheier, Int. J. Mass Spectrom. **271**, 15 (2008).
[16] S. L. Lunt, D. Field, J.-P. Ziesel, N. C. Jones, and R. J. Gulley, Int. J. Mass Spectrom. **205**, 197 (2001).
[17] K. Takatsuka and V. McKoy, Phys. Rev. A **24**, 2473 (1981).
[18] K. Takatsuka and V. McKoy, Phys. Rev. A **30**, 1734 (1984).
[19] M. A. P. Lima, L. M. Brescansin, A. J. R. da Silva, C. Winstead, and V. McKoy, Phys. Rev. A **41**, 327 (1990).
[20] M. H. F. Bettega, L. G. Ferreira, and M. A. P. Lima, Phys. Rev. A **47**, 1111 (1993).
[21] W. J. Hunt and W. A. Goddard III, Chem. Phys. Lett. **3**, 414 (1969).
[22] [http://cccbdb.nist.gov/].
[23] B. M. Bode and M. S. Gordon, J. Mol. Graphics Modell. **16**, 133 (1998).
[24] G. B. Bachelet, D. R. Hamann, and M. Schlüter, Phys. Rev. B **26**, 4199 (1982).
[25] M. H. F. Bettega, A. P. P. Natalense, M. A. P. Lima, and L. G. Ferreira, Int. J. Quantum Chem. **60**, 821 (1996).
[26] T. H. Dunning Jr., J. Chem. Phys. **53**, 2823 (1970).
[27] R. F. da Costa, F. J. da Paixão, and M. A. P. Lima, J. Phys. B **37**, L129 (2004); **38**, 4363 (2005).
[28] P. Chaudhuri, M. T. do N. Varella, C. R. C. de Carvalho, and M. A. P. Lima, Phys. Rev. A **69**, 042703 (2004).
[29] R. D. J. Nelson, D. R. J. Lide, and A. A. Maryott, Natl. Stand. Ref. Data Ser., Natl. Bur. Stand. (US) 10 (1967).
[30] M. A. Khakoo *et al.*, Phys. Rev. A **77**, 042705 (2008).
[31] S. d'A. Sanchez, F. Arretche, and M. A. P. Lima, Phys. Rev. A **77**, 054703 (2008).
[32] C. Winstead and V. McKoy, Phys. Rev. A **57**, 3589 (1998).
[33] C. W. Bauschlicher, J. Chem. Phys. **72**, 880 (1980).
[34] M. W. Schmidt *et al.*, J. Comput. Chem. **14**, 1347 (1993).
[35] K. Aflatooni, G. A. Gallup, and P. D. Burrow, J. Chem. Phys. **132**, 094306 (2010).
[36] K. Aflatooni, G. A. Gallup, and P. D. Burrow, J. Phys. Chem. A **104**, 7359 (2000).